

# Design, Fabrication, and Characterization of a Helical Twisting, Contracting, and Bending Fabric Soft Continuum Actuator

Pham H. Nguyen<sup>+</sup>, Imran I. B. Mohd<sup>+</sup>, Katherine Duford,  
Xiong Bao, and Wenlong Zhang\*, *Member, IEEE*

**Abstract**—In recent years, soft robots have demonstrated the capability for delicate and compliant interactions with objects, users, and unstructured environments. These soft robotic systems are bio-inspired from various examples like snakes, hydrostatic muscles in elephants and octopi, plant tendrils, etc. These soft actuation systems, like their biological counterpart have shown the ability to replicate natural movement, making them potentially effective in real world use cases. In this paper, we propose a new fabric-based soft continuum actuator with three chambers capable of helical twisting and simultaneous linear contraction as well as bending in multi-DOF. We characterize the performance of the system based on their geometrical parameters and preliminarily evaluate the system as a bionic winding manipulator and a soft robot arm.

## I. INTRODUCTION

Soft continuum robots that are capable of performing multi-degree of freedom (multi-DOF) manipulation have been a very popular sub-topic within the soft robotics community [1], [2]. This sub-field of soft robotics is inspired by muscular hydrostats found in elephant trunks and octopus arms [3]. Each muscular hydrostat unit is composed of transverse, longitudinal, and oblique muscle fiber arrangements that allow the arms to bend, elongate, shorten, or twist [3]. Because of the innate nature of intrinsically soft actuators, combinations these actuators can theoretically reach an infinite DOF. Various types of actuators have been utilized to soft continuum robots, including pneumatic artificial muscles [4]–[7], origami [8]–[11], cable-driven systems [12]–[15], elastomeric [16]–[21], and fabric [22]–[27] actuators.

Currently, most soft continuum actuation units have limited motion capabilities when compared to a muscular hydrostat, since increasing the DOF of each soft actuation unit leads to increased weights and control complexities. Thus there is still a need to design a soft actuation unit that can perform diverse functions without adding actuators.

In our previous work, we highlighted the versatility of creating soft continuum actuators, based on elastomeric and

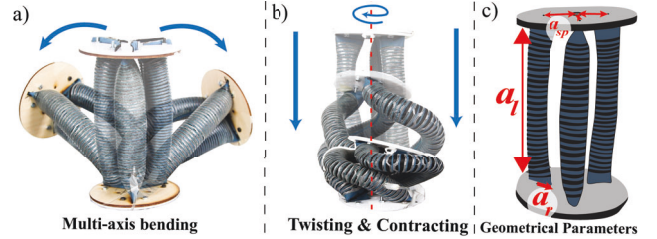


Fig. 1: Fabric Soft Continuum Actuator. (a) Multi-axis bending motion. (b) Helical twisting and contraction motion. (c) The geometrical parameters: length of the actuators ( $a_l$ ), the radius of the actuators ( $a_r$ ), and the spacing between the actuators and the center of the module ( $a_{sp}$ ).

woven fabrics [16], [23]. These designs focused on creating multi-axis bending motions. More recently, we introduced a knit-fabric based soft continuum actuator capable of multi-axis bending, bi-directional twisting, and extending [28].

In this paper, we created a soft continuum multi-actuator system capable of performing multi-axis bending, helical twisting, and contracting by utilizing only three bending knit fabric reinforced textile actuators (knit FRTAs) [29], as seen in Fig. 1. From previous work and nature, torsioning is an important capability for animals and humans to achieve more complex spatial positioning quickly. Various types of torsional actuators exist including fiber weave actuators [30]–[32], antagonistic actuators [33], rotary pneumatic actuators [34]–[37], and pleated chamber actuators [30], [38]. Unlike previous work, this soft continuum actuator system is not mechanically programmed for twisting with fibers, chambers, or pleats. The proposed approach enables twisting coupled with contracting by utilizing only bending FRTAs, which are already capable of multi-axis bending.

In this work, we demonstrate how this module is designed and further study the behavior of the system by monitoring its twisting and contracting performance. We demonstrate its capabilities by grasping objects utilizing bionic winding [39]. This work highlights the possibility of creating a helically twisting and contracting soft continuum module, which is still capable of multi-axis bending without utilizing dedicated twisting actuators. Thus, highlighting the possibility of building soft continuum modules with expansive number of DOFs, without increasing the design complexity.

## II. DESIGN

In this work, each soft continuum robotic module includes three bending FRTAs, as seen in Fig. 1. The fabrication process of this actuator is highlighted in our previous

This work was supported in part by the National Science Foundation under Grant CMMI-1800940.

P. Nguyen was with the Polytechnic School, Arizona State University. He is currently with Aerial Robotics Laboratory, Department of Aeronautics, Imperial College London, UK. [n.pham@imperial.ac.uk](mailto:n.pham@imperial.ac.uk)

I. Mohd, K. Duford, and X. Bao are with School for Engineering of Matter, Transport and Energy, Ira A. Fulton Schools of Engineering, Arizona State University, Tempe, AZ 85281, USA.

W. Zhang is with the Polytechnic School, Ira A. Fulton Schools of Engineering, Arizona State University, Mesa, AZ 85212, USA. [wenlong.zhang@asu.edu](mailto:wenlong.zhang@asu.edu)

<sup>+</sup> P. H. Nguyen and Imran I. B. Mohd are equally contributing authors.

\* Address all correspondence to this author.

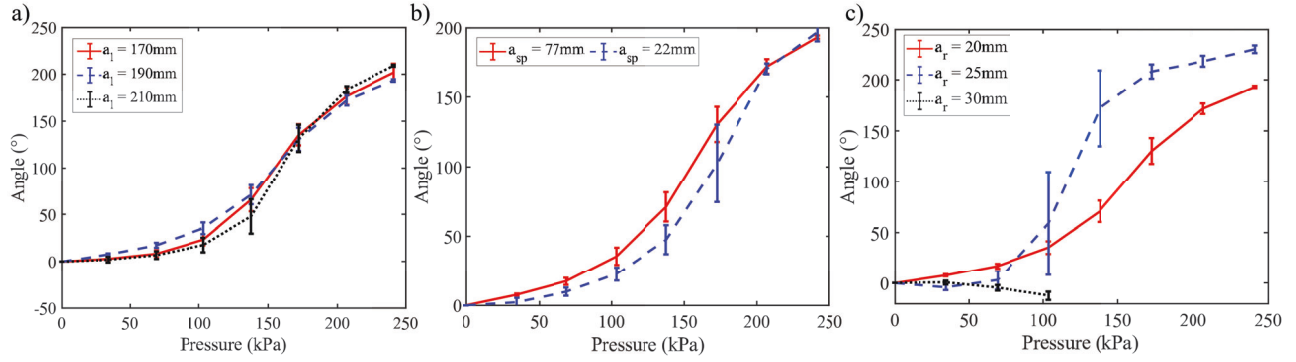


Fig. 2: Twisting mobility based on: (a) Actuator length ( $a_l$ ). (b) Actuator spacing ( $a_{sp}$ ). (c) Actuator radius ( $a_r$ ).

work [29]. This setup naturally allows the module to bend in multi-directions, by inflating a single actuator or two adjacent actuators. The difference between this module and our previous work [28], is that by inflating all the three actuators together, a helical twisting and contracting motion occurs, instead of an extension motion. We believe that this motion occurs because the inextensible sewing line on each actuator eliminates the ability for the actuator to extend. This leads the three actuators to bend in three different directions, promoting a rotational motion on the top plate and forces a twisting helical motion as the soft body of the actuators collapse at the same time.

### III. CHARACTERIZATION AND EVALUATION

We further evaluated the performance of the module by varying the system's geometrical parameters, highlighted in Fig. 1c. The length of the actuators ( $a_l$ ) was evaluated for lengths of 170, 190, and 210 mm. The spacing ( $a_{sp}$ ) between the three actuators was evaluated for 22 and 77 mm. The radius of the actuators ( $a_r$ ) was varied between 20, 25, and 30 mm.

In Figs. 2c, 3c and 3f, we noticed that after 103.4kPa, the actuators of the module with  $a_r = 30mm$ , started showing uncontrolled radial expansion leading to failure and the thread on the seam started peeling, before any significant twisting and contracting motion occurred.

All the payload tests were performed on a Universal Tensile Machine (Instron 5944; Instron Corp., High Wycombe, UK). For the mobility tests, two sets of passive markers were mounted at the base and top plates of the module. The markers were recorded utilizing a motion capture system (Optitrack, NaturalPoint Inc., Corvallis, OR). Each experiment was repeated three times and the actuators in the module were inflated at a pressure interval of 34.5kPa.

#### A. Bending Performance

In the bending test,  $a_{sp}$  was set at 77 mm,  $a_r = 25mm$ , and the length of the actuator,  $a_l$  was set at 190mm. Only a single bending actuator on the module was inflated up to 241.3kPa. The module's maximum bending payload with a single bending actuator inflated was  $7.63 \pm 1.2$  N and the maximum bending angle noticed was  $148.7 \pm 0.61^\circ$ .

#### B. Twisting Performance

By varying the length of the actuators ( $a_l$ ), the module was able to twist up to  $201.62 \pm 9.33^\circ$ ,  $193.14 \pm 1.17^\circ$ ,  $208.99 \pm 1.08^\circ$  at 241.3kPa, respectively. We notice that the twisting performance of the module was unaffected by the change in length of the actuators, as seen in Fig. 2a.

Varying the spacing between the actuators, as shown in Fig. 2b, did not affect the final twisting angle of the actuator at 241.3kPa. However, it was noticed that by placing the actuators slightly further apart at  $a_{sp} = 77mm$ , the module was twisting more until about 206.8kPa.

For actuators with a radius of  $a_r = 20mm$  and  $a_r = 25mm$ , the twisting angles at 241.3kPa were  $193.14 \pm 1.17^\circ$  and  $230.36 \pm 3.70^\circ$  respectively. The actuator with a radius of  $a_r = 25mm$  showed a better overall twisting performance. Therefore, the maximum actuator radius for an actuator with a length of 190mm, is approximately 25mm.

#### C. Contracting Performance

By varying  $a_l$ , it highlighted similar contraction length between modules with  $a_l = 190mm$  and  $a_l = 210mm$ , with contraction of  $102.28 \pm 1.08mm$  and  $97.10 \pm 0.46mm$  at 241.3kPa, respectively, as seen in Fig. 3a. However, the module with  $a_l = 170mm$  only had a contraction length of  $77.77 \pm 1.47mm$ .

The change in  $a_l$  also affected the contraction force of the module, as seen in Fig. 3d. The maximum contraction payload capacity was respectively  $16.89 \pm 1.73N$ ,  $22.07 \pm 0.28N$ , and  $19.8667 \pm 0.48N$  for  $a_l = 170mm$ , 190mm and 210mm, respectively. It should be noted that before creating a contraction pulling force, the module extends very slightly, creating a pushing force of  $-27.5 \pm 1.11N$ ,  $-27.2 \pm 0.48N$  and  $-14.1 \pm 0.83N$ , respectively. This highlights that the module with the longest actuators ( $a_l = 210mm$ ), shows the least pushing force before starting to contract.

As shown in Fig. 3b, the larger the spacing distance between the actuators the more the module seems to contract. At 206.8kPa, the module with  $a_{sp} = 22mm$  and  $a_{sp} = 77mm$  had the contracting lengths of  $89.37 \pm 3.78mm$  and  $102.28 \pm 1.09mm$ , respectively. The change in spacing between the actuators,  $a_{sp}$ , showed less of an affect on the contraction force of the module, seen in Fig. 3e. Thus the modules with  $a_{sp} = 22mm$  and  $a_{sp} = 77mm$  had contract forces of  $24 \pm 1.29N$  and  $22.07 \pm 0.28N$ , respectively.

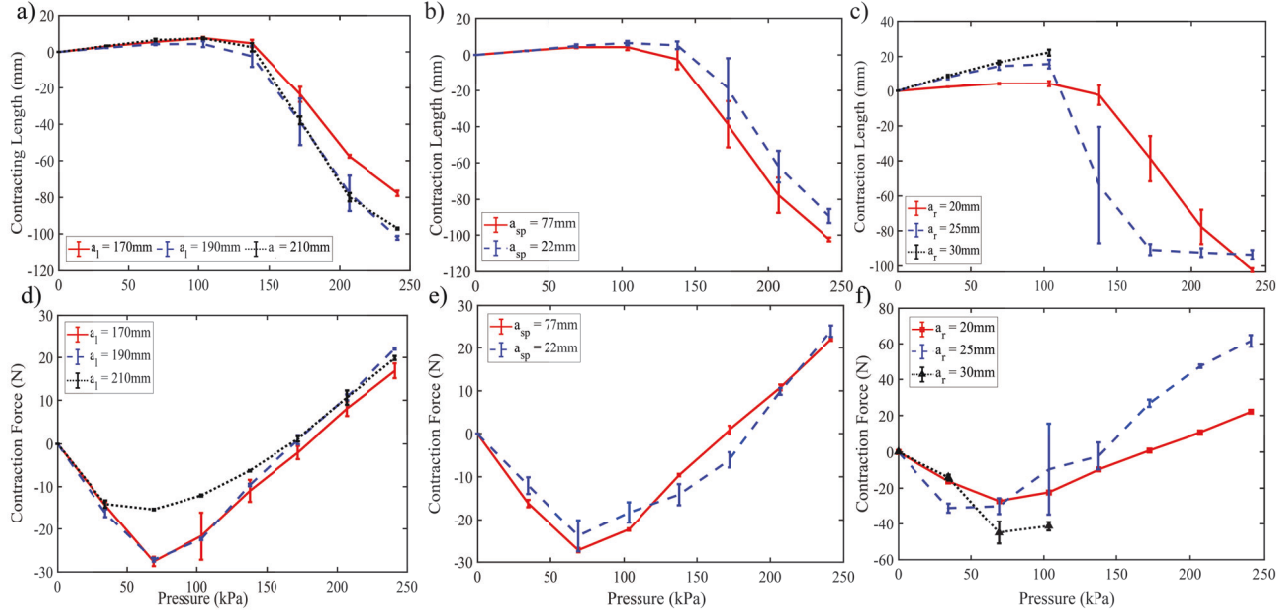


Fig. 3: Contracting mobility based on: (a) Actuator length ( $a_l$ ). (b) Actuator spacing ( $a_{sp}$ ). (c) Actuator radius ( $a_r$ ). Contracting payload based on: (d) Actuator length ( $a_l$ ). (e) Actuator spacing ( $a_{sp}$ ). (f) Actuator radius ( $a_r$ ).

Similarly to the twisting performance, we noticed that the module with largest actuator radius ( $a_r = 30mm$ ) was not able to contract as the pressure increased as well, seen in Fig. 3c. We also noticed that the module with  $a_r = 20mm$  and  $a_r = 25mm$  had contracting lengths of  $102.28 \pm 1.09mm$  and  $93.71 \pm 2.67mm$  at  $241.3kPa$ , respectively. The module with  $a_r = 25mm$  achieved the maximum contracting length earlier at  $172.4kPa$ , showing a better overall contracting mobility performance.

As the module with the largest actuator radius was not able to contract, we did not see a change in contraction force of that module, as seen in Fig. 3f. We also saw a larger contraction force of  $61.65 \pm 3.33N$  for the module with  $a_r = 25mm$  compared to the module with  $a_r = 20mm$  with a contraction force of  $22.07 \pm 0.28N$  at  $241.3kPa$ .

#### D. Preliminary Evaluation of the Soft Continuum Module Applications

1) *Bionic Winding Manipulator*: The twisting and contracting motion profile of the module highlighted a unique

grasping methodology using bionic winding, as seen in Fig. 4. The grasping performance of the module was preliminarily evaluated by grasping three different types of objects with different weights, sizes and textures: a ball, a wooden block, and a plastic water bottle, shown in Figs. 4a-c.

2) *Soft Robotic Wrist*: We also highlight the module as a soft robotic wrist by twisting to uncup and cap a bottle, as seen in Fig. 4d. A plate with a cut out with the same radius of the bottle cap was attached to the end of the actuator. When the module is pressed against the bottle cap a snug fit is established. Then by inflating the actuators the module twists to uncup the bottle in a counter-clockwise motion. To cap the bottle again, the actuators in the module are deflated, creating a clockwise motion.

3) *Soft Continuum Robotic Arm*: To assemble the soft continuum robot arm (SCRA) the connector pieces at the end of each soft module were designed to easily attach and detach to each other using nuts and bolts. The modules were made of actuators with a length of  $190mm$ , to combine to create a SCRA with a length of approximately  $590mm$ . In this work, the SCRA was preliminarily evaluated for bending and contracting, as seen in Fig. 4e. The full arm was able to contract to approximately  $301mm$  (48.98% contraction).

#### IV. CONCLUSION

In this paper, we presented the design, characterization, and preliminary evaluation of a new soft continuum module that utilized only 3 actuators to be able to perform multi-axis bending and a coupled motion of helical twisting and contracting. The geometrical parameters of the module were explored as a guideline on how the length and radius of the actuators and spacing between them affect the motion and payload of the module, when inflated with an input pressure. This actuator was also used to build a bionic winding manipulator and soft continuum robot arm.

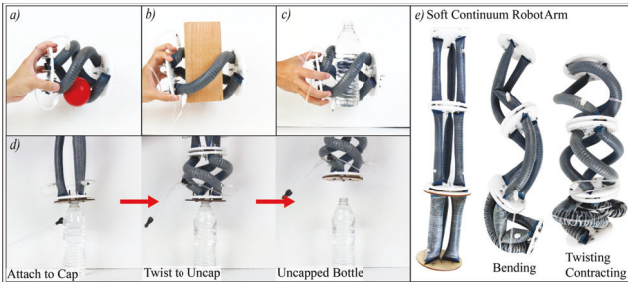


Fig. 4: Preliminary evaluation of the module. (a) Grasping a ball (25.7g). (b) Grasping a wood block (240.5g). (c) grasping a bottle (500.4g). (d) Uncapping and Capping a water bottle. (e) The soft continuum robot arm.



## REFERENCES

- [1] T. George Thuruthel, Y. Ansari, E. Falotico, and C. Laschi, "Control strategies for soft robotic manipulators: A survey," *Soft Robotics*, vol. 5, no. 2, pp. 149–163, 2018.
- [2] J. Burgner-Kahrs, D. C. Rucker, and H. Choset, "Continuum robots for medical applications: A survey," *IEEE Transactions on Robotics*, vol. 31, no. 6, pp. 1261–1280, 2015.
- [3] W. Kier and K. Smith, "The biomechanics of movement in tongues and tentacles," *Journal of Biomechanics*, vol. 16, no. 4, pp. 292–293, 1983.
- [4] I. S. Godage, G. A. Medrano-Cerda, D. T. Branson, E. Guglielmino, and D. G. Caldwell, "Dynamics for variable length multisection continuum arms," *The International Journal of Robotics Research*, vol. 35, no. 6, pp. 695–722, 2016.
- [5] Q. Guan, J. Sun, Y. Liu, N. M. Wereley, and J. Leng, "Novel bending and helical extensile/contractile pneumatic artificial muscles inspired by elephant trunk," *Soft Robotics*, 2020.
- [6] P. Ohta, L. Valle, J. King, K. Low, J. Yi, C. G. Atkeson, and Y.-L. Park, "Design of a lightweight soft robotic arm using pneumatic artificial muscles and inflatable sleeves," *Soft Robotics*, vol. 5, no. 2, pp. 204–215, 2018.
- [7] J. D. Greer, T. K. Morimoto, A. M. Okamura, and E. W. Hawkes, "Series pneumatic artificial muscles (spams) and application to a soft continuum robot," in *2017 IEEE International Conference on Robotics and Automation (ICRA)*. IEEE, 2017, pp. 5503–5510.
- [8] T. Liu, Y. Wang, and K. Lee, "Three-dimensional printable origami twisted tower: Design, fabrication, and robot embodiment," *IEEE Robotics and Automation Letters*, vol. 3, no. 1, pp. 116–123, Jan 2018.
- [9] J. Santoso and C. D. Onal, "An origami continuum robot capable of precise motion through torsionally stiff body and smooth inverse kinematics," *Soft Robotics*, 2020.
- [10] M. A. Robertson, O. C. Kara, and J. Paik, "Soft pneumatic actuator-driven origami-inspired modular robotic 'pneumagami'," *The International Journal of Robotics Research*, p. 0278364920909905, 2020.
- [11] K. Zhang and K. Althoefer, "Designing origami-adapted deployable modules for soft continuum arms," in *Annual Conference Towards Autonomous Robotic Systems*. Springer, 2019, pp. 138–147.
- [12] W. McMahan, B. A. Jones, and I. D. Walker, "Design and implementation of a multi-section continuum robot: Air-octor," in *2005 IEEE/RSJ International Conference on Intelligent Robots and Systems*. IEEE, 2005, pp. 2578–2585.
- [13] T. Kato, I. Okumura, S.-E. Song, A. J. Golby, and N. Hata, "Tendon-driven continuum robot for endoscopic surgery: Preclinical development and validation of a tension propagation model," *IEEE/ASME Transactions on Mechatronics*, vol. 20, no. 5, pp. 2252–2263, 2014.
- [14] K. Oliver-Butler, J. Till, and C. Rucker, "Continuum robot stiffness under external loads and prescribed tendon displacements," *IEEE Transactions on Robotics*, vol. 35, no. 2, pp. 403–419, 2019.
- [15] M. Li, R. Kang, S. Geng, and E. Guglielmino, "Design and control of a tendon-driven continuum robot," *Transactions of the Institute of Measurement and Control*, vol. 40, no. 11, pp. 3263–3272, 2018.
- [16] P. H. Nguyen, C. Sparks, S. G. Nuthi, N. M. Vale, and P. Polygerinos, "Soft Poly-Limbs: Toward a New Paradigm of Mobile Manipulation for Daily Living Tasks," *Soft Robotics*, p. soro.2018.0065, 2018.
- [17] C. Della Santina, R. K. Katzschmann, A. Bicchi, and D. Rus, "Model-based dynamic feedback control of a planar soft robot: Trajectory tracking and interaction with the environment," *The International Journal of Robotics Research*, vol. 39, no. 4, pp. 490–513, 2020.
- [18] A. D. Marchese and D. Rus, "Design, kinematics, and control of a soft spatial fluidic elastomer manipulator," *The International Journal of Robotics Research*, vol. 35, no. 7, pp. 840–869, 2016.
- [19] J. Bishop-Moser, G. Krishnan, C. Kim, and S. Kota, "Design of soft robotic actuators using fluid-filled fiber-reinforced elastomeric enclosures in parallel combinations," in *2012 IEEE/RSJ International Conference on Intelligent Robots and Systems*. IEEE, 2012, pp. 4264–4269.
- [20] S. Kurumaya, B. T. Phillips, K. P. Becker, M. H. Rosen, D. F. Gruber, K. C. Galloway, K. Suzumori, and R. J. Wood, "A modular soft robotic wrist for underwater manipulation," *Soft robotics*, vol. 5, no. 4, pp. 399–409, 2018.
- [21] Z. Gong, B. Chen, J. Liu, X. Fang, Z. Liu, T. Wang, and L. Wen, "An opposite-bending-and-extension soft robotic manipulator for delicate grasping in shallow water," *Frontiers in Robotics and AI*, vol. 6, p. 26, 2019.
- [22] H. Lee, N. Oh, and H. Rodrigue, "Expanding pouch motor patterns for programmable soft bending actuation: Enabling soft robotic system adaptations," *IEEE Robotics Automation Magazine*, vol. 27, no. 4, pp. 65–74, 2020.
- [23] P. H. Nguyen, I. I. Mohd, C. Sparks, F. L. Arellano, W. Zhang, and P. Polygerinos, "Fabric soft poly-limbs for physical assistance of daily living tasks," in *2019 International Conference on Robotics and Automation (ICRA)*. IEEE, 2019, pp. 8429–8435.
- [24] C. M. Best, M. T. Gillespie, P. Hyatt, L. Rupert, V. Sherrod, and M. D. Killpack, "A new soft robot control method: Using model predictive control for a pneumatically actuated humanoid," *IEEE Robotics Automation Magazine*, vol. 23, no. 3, pp. 75–84, Sep. 2016.
- [25] X. Liang, H. Cheong, Y. Sun, J. Guo, C. K. Chui, and C. Yeow, "Design, Characterization and Implementation of a Two - DOF Fabric - based Soft Robotic Arm," *IEEE Robotics and Automation Letters*, vol. 3766, no. c, pp. 1–8, jul 2018.
- [26] M. Hofer and R. D'Andrea, "Design, fabrication, modeling and control of a fabric-based spherical robotic arm," *Mechatronics*, vol. 68, p. 102369, 2020.
- [27] H. D. Yang and A. T. Asbeck, "A new manufacturing process for soft robots and soft/rigid hybrid robots," in *2018 IEEE/RSJ International Conference on Intelligent Robots and Systems (IROS)*. IEEE, 2018, pp. 8039–8046.
- [28] P. H. Nguyen, Z. Qiao, S. Seidel, S. Amatya, I. I. B. Mohd, and W. Zhang, "Towards an untethered knit fabric soft continuum robotic module with embedded fabric sensing," in *2020 3rd IEEE International Conference on Soft Robotics (RoboSoft)*, 2020, pp. 615–620.
- [29] P. H. Nguyen and W. Zhang, "Design and computational modeling of fabric soft pneumatic actuators for wearable assistive devices," *Scientific reports*, vol. 10, no. 1, pp. 1–13, 2020.
- [30] S. Sanan, P. S. Lynn, and S. T. Griffith, "Pneumatic Torsional Actuators for Inflatable Robots," *Journal of Mechanisms and Robotics*, vol. 6, no. 3, p. 031003, 2014.
- [31] F. Connolly, P. Polygerinos, C. J. Walsh, and K. Bertoldi, "Mechanical programming of soft actuators by varying fiber angle," *Soft Robotics*, vol. 2, no. 1, pp. 26–32, 2015.
- [32] L. H. Blumenschein, N. S. Usevitch, B. H. Do, E. W. Hawkes, and A. M. Okamura, "Helical actuation on a soft inflated robot body," in *2018 IEEE International Conference on Soft Robotics (RoboSoft)*, 2018, pp. 245–252.
- [33] J. Yan, X. Zhang, B. Xu, and J. Zhao, "A new spiral-type inflatable pure torsional soft actuator," *Soft robotics*, vol. 5, no. 5, pp. 527–540, 2018.
- [34] A. Ainla, M. S. Verma, D. Yang, and G. M. Whitesides, "Soft, rotating pneumatic actuator," *Soft robotics*, vol. 4, no. 3, pp. 297–304, 2017.
- [35] Z. Jiao, C. Ji, J. Zou, H. Yang, and M. Pan, "Vacuum-powered soft pneumatic twisting actuators to empower new capabilities for soft robots," *Advanced Materials Technologies*, vol. 4, no. 1, p. 1800429, 2019.
- [36] X. Gong, K. Yang, J. Xie, Y. Wang, P. Kulkarni, A. S. Hobbs, and A. D. Mazzeo, "Rotary actuators based on pneumatically driven elastomeric structures," *Advanced Materials*, vol. 28, no. 34, pp. 7533–7538, 2016.
- [37] J. Fras, Y. Noh, H. Wurdemann, and K. Althoefer, "Soft fluidic rotary actuator with improved actuation properties," in *2017 IEEE/RSJ International Conference on Intelligent Robots and Systems (IROS)*. IEEE, 2017, pp. 5610–5615.
- [38] H. Amase, Y. Nishioka, and T. Yasuda, "Mechanism and basic characteristics of a helical inflatable gripper," in *2015 IEEE International Conference on Mechatronics and Automation (ICMA)*, 2015, pp. 2559–2564.
- [39] H. Li, J. Yao, P. Zhou, X. Chen, Y. Xu, and Y. Zhao, "High-load soft grippers based on bionic winding effect," *Soft robotics*, vol. 6, no. 2, pp. 276–288, 2019.